Observations of fast protons above 1 MeV produced in direct-drive laser-fusion experiments

D. G. Hicks,[a] C. K. Li, F. H. Séguin, J. D. Schnittman, A. K. Ram, J. A. Frenje, and R. D. Petrasso[b]
Plasma Science and Fusion Center, Massachusetts Institute of Technology, Massachusetts 02139

J. M. Soures, D. D. Meyerhofer, S. Roberts, C. Sorce, and C. Stöckl
Laboratory for Laser Energetics, University of Rochester, Rochester, New York 14623

T. C. Sangster and T. W. Phillips
Lawrence Livermore National Laboratory, Livermore, California 94550

(Received 26 April 2000; accepted 1 November 2000)

Fast protons $\gtrsim 1$ MeV have been observed on the 60-beam, 30 kJ OMEGA laser [T. R. Boehly *et al.*, Opt. Commun. **133**, 495 (1997)] at an intensity $I \simeq 10^{15}$ W/cm^2 and a wavelength $\lambda = 0.35$ μm. These energies are more than 5 times greater than those observed on previous, single-beam experiments at the same $I\lambda^2$. The total energy in the proton spectrum above 0.2 MeV is $\sim 0.1\%$ of the laser energy. Some of the proton spectra display intense, regular lines which may be related to ion acoustic perturbations in the expanding plasma. © *2001 American Institute of Physics.* [DOI: 10.1063/1.1335831]

I. INTRODUCTION

The production of ions at suprathermal energies during high-intensity laser interactions with solids has been observed in many previous experiments.[1–6] Such accelerated ions, or fast ions, are associated with hot electrons which produce electrostatic fields through charge separation.[7–9]

Studies using time-of-flight detectors have shown that the highest velocity particles produced in laser–solid interactions are always protons,[3] regardless of the type of target material. These protons have been examined extensively and a characteristic feature of their spectra is the presence of a well-defined, maximum cutoff energy, $E_p^{\max}$. A number of studies have indicated that $E_p^{\max}$ is a function only of $I\lambda^2$ and follows the scaling relation given by[1,2,6,10]

$$E_p^{\max} = 3.51 \times 10^{-6} (I\lambda^2)^{1/3}, \tag{1}$$

covering the range $I\lambda^2 = 10^{14} - 10^{19}$ Wcm^{-2}μm^2, where $E_p^{\max}$ is the maximum proton energy in MeV, I is the laser intensity in Wcm^{-2}, and λ is the laser wavelength in μm. This scaling, which is applicable over five orders-of-magnitude in intensity, was established by experiments utilizing a wide variety of laser energies, wavelengths, spot sizes, and target materials. In addition, the use of at least three different types of diagnostic systems indicated that the measurements were not an artifact of specific detector sensitivities.

It is important to note, however, that this scaling was developed strictly for protons produced in laser–solid interactions (or, more accurately, laser interactions with solid-density plasmas) as is relevant to the experiments to be described below. It is not directly applicable to multiply-charged ions[4] (whose maximum energies, for high charge states, may be greater than that of the protons) or to laser interactions with atomic clusters[11,12] or underdense plasmas,[13,14] which produce ion energies less than, or, for some high-Z atomic cluster studies,[11] approaching those given by Eq. (1).

In this article we describe measurements of fast protons produced by irradiating solid targets with the 60-beam, 30 kJ OMEGA laser used in direct-drive laser-fusion experiments.[15] This laser system represents a new environment for fast-ion studies since no previous experiments have been performed on a system with such a large number of overlapping beams. Results show that proton energies under these conditions are more than 5 times greater than would be expected from the experimentally-derived scaling given by Eq. (1). In addition, high-resolution spectroscopy reveals the presence of intense, regular spectral lines superimposed upon the expected exponential-like velocity spectra. To the best of our knowledge, no such features have ever been observed before, perhaps due to the lower resolution of previous spectral measurements.[1,16]

Although some speculation about the source of the enhanced acceleration and spectral lines will be presented, a thorough interpretation of these phenomena is still unavailable. The following discussion will thus focus primarily on presenting the nature and character of these observations.

II. EXPERIMENTS

The experiments were performed on the OMEGA laser system at the Laboratory for Laser Energetics, University of Rochester. OMEGA is a 60-beam, neodymium-doped phosphate glass laser capable of delivering 30 kJ of frequency-tripled, 0.35 μm light.[15] Irradiation uniformity is accomplished using distributed phase plates and smoothing by spectral dispersion (SSD) with a bandwidth of 0.2 THz.[17] Including the effects of beam-to-beam energy variations, the

[a]Present address: Lawrence Livermore National Laboratory, Livermore, California 94550. Electronic mail: hicks13@llnl.gov
[b]Visiting Senior Scientist at the Laboratory for Laser Energetics, University of Rochester, Rochester, New York 14623.

estimated illumination uniformity for 60 overlapping beams was ~5%–10%. For these studies, laser pulse shapes were mostly 1 ns square, with a few 1 ns Gaussian pulses and 0.4 ns square pulses. On spherical targets, the laser beams were focused to nearly tangentially illuminate the target at the beam edge, delivering total energies on target between 8 to 30 kJ. Laser intensities varied from 10^{14} to 10^{15} Wcm^{-2}, where the intensity is calculated by dividing the total incident laser energy by the pulse length and initial target surface area. Targets were mostly 0.9–1 mm diameter spherical microballoons with glass or paralene (CH) shell material ranging from 2 to 20 μm in thickness. Some shells consisted of a few microns of CH overlaying a few microns of glass. Targets were generally filled with some combination of deuterium, tritium, or ^{3}He fuel. In addition to these spherical microballoons, two flat-foil targets, composed of 1200 μm of CH, were illuminated with 38 beams on one side. Average laser intensities for these shots were 5.2×10^{14} and 6.4×10^{14} Wcm^{-2}.

Spectra were observed primarily using a charged-particle spectrometer[18] consisting of a 7.6 kG permanent magnet with CR-39 nuclear track-etch detectors. The instrument is capable of measuring the spectra of both fast ions and higher energy fusion products, and has a total energy range extending from 0.1 to 40 MeV. Use of a high-field magnet in conjunction with single-particle discrimination from track detectors gives this instrument high energy resolution, better than 1% over the energy range for fast ions, or $\lesssim$3 keV at 500 keV. Systematic uncertainties are $<2\%$. A rapid, automated scanning system was developed which can readily count 10^6 tracks per shot. Simultaneous measurements are made by two virtually identical spectrometers positioned 101° apart, one outside the OMEGA chamber at 235 cm from the target (CPS-1), the other inside at 100 cm (CPS-2).

It is important to note that by utilizing a magnet in conjunction with CR-39, this spectrometer has the ability to uniquely identify all particle species of current interest, i.e., fast protons (for this study) and charged fusion products (for studies described elsewhere[19,20]) without the need for a Thomson parabola. This is because particles of different species which have the same gyroradius (and thus land at the same detector position) produce different size tracks. Track sizes have been calibrated from particle sources of known energy and a track-growth model developed to predict the size of all other relevant particles. In particular, protons can always be discriminated from heavier ions since proton track sizes are the smallest for any given gyroradius. For convenience, most of the heavier fast ion species, such as different charge states of carbon, are removed with a few microns of aluminum filtering in front of the CR-39.

For a few shots where the spectrometer was not available, maximum proton energies were determined using CR-39 in conjunction with ranging filters. These consisted of pieces of CR-39 mounted normal to the target direction and covered in different regions by aluminum filters of various thicknesses. The maximum fast proton energy was determined by finding which filter thickness was required to remove the proton signal. Protons were easily identified by their small track sizes. With the discrete thicknesses, the uncertainty in this cutoff energy measurement was about 0.1 MeV—substantially greater than the uncertainty in the spectrometer measurements. In the following results, ranging filter data is used only to determine the maximum proton energy and not any other spectral information.

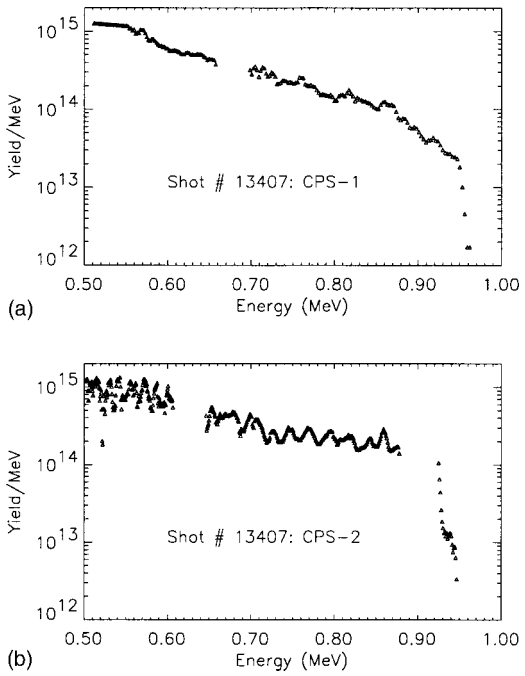

FIG. 1. Fast proton spectra for a single shot measured concurrently by the two spectrometers, CPS-1 (at 235 cm) and CPS-2 (at 100 cm). The gaps are due to spaces between adjacent pieces of CR-39 covering the magnet dispersion region. Total particle yield per MeV is inferred by dividing the measured counts by the fractional solid angle subtended by each spectrometer. Although the spectral shapes on a single shot measured by each instrument can differ quite substantially (as do the total particle yield and energy), the endpoint energies are approximately equal.

III. RESULTS AND DISCUSSION

Sample fast proton spectra obtained simultaneously by each spectrometer are illustrated in Fig. 1, clearly showing the characteristic maximum cutoff energy.[21] Despite different spectral shapes, the endpoint energies observed from both views are approximately equal and are generally within 50 keV of each other (where the systematic error between instruments is $<$40 keV). Slight asymmetries in endpoint energies have been observed on some shots.

In addition to the fast protons, charged fusion products have been measured and observed with energy upshifts of ~0.5 MeV. The acceleration of these fusion particles is treated elsewhere.[19]

The measurements of maximum proton energy are plotted versus $I\lambda^2$ in Fig. 2. The scaling given in Eq. (1) is shown by the dotted line for comparison. For $I\lambda^2<2\times10^{13}$ $\mathrm{Wcm}^{-2}\mu\mathrm{m}^2$, the proton energies are below the detectable limit of 100 keV, while at $I\lambda^2=1.2\times10^{14}$ $\mathrm{Wcm}^{-2}\mu\mathrm{m}^2$ energies up to 1.4 MeV were observed. Neither laser-pulse duration (at 0.4 or 1 ns), pulse shape (square or Gaussian), nor application of SSD appeared to make any substantial difference to the maximum proton en-

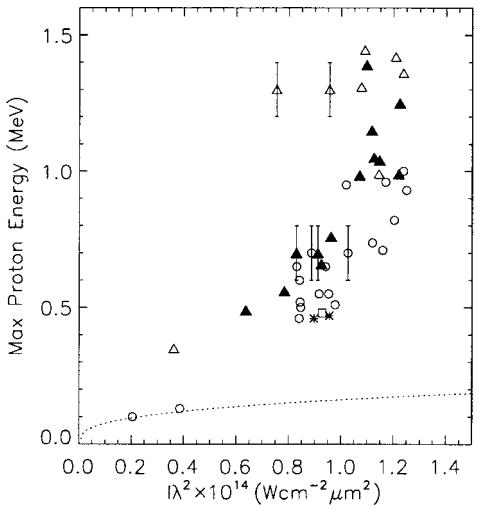

FIG. 2. Scaling of maximum fast-proton energy with $I\lambda^2$. Open circles and asterisks are for glass shells with 1 and 0.4 ns pulses, respectively. Solid triangles and the square are for CH shells >5 μm thick with 1 and 0.4 ns pulses, respectively. The open triangles are for CH shells <5 μm thick with 1 ns pulses, including those with CH overlaying glass. Error bars are only shown for the ranging filter measurements since, for the CPS data, errors are $<2\%$ and are smaller than the plot symbols. The scaling given in Eq. (1) is shown as a dotted line for reference.

ergies. When observed from both spectrometers simultaneously, the difference in maximum proton energy was less than 50 keV (slightly larger than the systematic error between the two spectrometers), showing that asymmetries are typically less than 5%. Results from the CR-39 and ranging filter detectors are consistent with those from the spectrometers.

Importantly, fast protons produced on the two flat foil targets composed of 1200 μm of CH and irradiated by 38 beams on a side (shown as solid triangles at $I\lambda^2$'s of 0.64×10^{14} and 0.78×10^{14} $\mathrm{Wcm}^{-2}\mu\mathrm{m}^2$) had maximum energies which followed the same scaling as the thick-shell CH spherical targets. This indicates that the geometry of the target does not appear to influence the fast proton emission energies.

On the other hand, as Fig. 2 shows, the type of target material does appear to influence the proton energies. Maximum energies were generally higher for targets with thin CH shells (<5 μm thick, whether or not the CH was overlaying glass) than they were for either glass or thicker CH shell targets. A single spherical gold target, irradiated at $I\lambda^2=10^{14}$ $\mathrm{Wcm}^{-2}\mu\mathrm{m}^2$ using 60 beams, produced no fast protons above 100 keV.

The scatter among the individual measurements for different shots is typically larger than can be explained by uncertainties in the instruments alone. This observation is typical for fast ion measurements of this kind and has also been observed elsewhere (see Fews *et al.*[6] and references therein). It is likely that variabilities in the laser conditions, such as beam-to-beam energy balance, local hot spots, prepulse levels, or ramp-up time play a role in this scatter.

As illustrated in Fig. 2, the measured proton energies of $\sim$ 1 MeV are more than 5 times greater than those observed previously at the same $I\lambda^2$.[1] In order to place the OMEGA measurements in context, it is useful to examine the repeatability of the previously-determined scaling with $I\lambda^2$ and whether or not there has been any precedence for such enhanced acceleration. The relationship given by Eq. (1) was determined by single-beam studies over four orders-of-magnitude in intensity using nanosecond pulses of 10.6 μm light at energies up to 1 kJ focused to spot sizes of $\sim$100 μm.[1] A similar scaling was found in the high-intensity range for single-beam experiments using picosecond pulses of 1.05 μm light at low energy (30 J) focused to spot sizes of $\sim$12 μm.[2] Despite the substantially different laser energies, wavelengths, and spot sizes of these two studies, there was no indication of any significant deviation from the scaling with $I\lambda^2$ given by Eq. (1). However, there was a difference when eight beams were used to illuminate the target instead of one, with a slightly stronger scaling with $I\lambda^2$ being observed on such multiple-beam experiments.[1,22] It is notable that these multi-beam experiments found that maximum proton energies were dependent on the target material whereas the single-beam experiments observed no such dependency. On the 60-beam OMEGA laser, we measure an even stronger scaling with $I\lambda^2$ than observed on the 8-beam studies and we find that glass and CH targets can lead to different maximum proton energies. Thus the only precedence for violation of the scaling given by Eq. (1) was found on multiple-beam experiments, indicating that it is perhaps the presence of 60 beams on OMEGA that is responsible for the elevated proton energies. It should be emphasized that laser conditions on OMEGA are unique in many other ways besides the presence of 60 beams and, without performing a systematic study, it is difficult to isolate any single responsible factor.

Since fast ions are generally thought to be associated with hot electrons driving the plasma expansion into vacuum,[7–9] it is instructive to infer an effective hot electron temperature from the proton spectra. To do this requires that a model be used to describe the plasma expansion. The simplest such description commonly used is the isothermal, self-similar model[7] which shows that the hot electron temperature, T_h, can be determined from the slope of the velocity spectrum. For our studies, the spectra do not always have a single, well-defined slope; however their character is generally exponential-like and by a least-squares fit to the velocity spectra (avoiding the steep endpoint region), the average slope and thus an effective temperature can be determined. In Fig. 3 the maximum proton energy is shown to be proportional to the inferred T_h, with a best fit giving the relationship $E_p^{\max}/T_h=55$. This value is close to the experimentally determined value of $E_p^{\max}/T_h=66$ found by Tan *et al.*[1] It is striking that, although the maximum proton energies, $E_p^{\max}$, do not follow the scaling with $I\lambda^2$ found on previous experiments, they do appear to follow the scaling with T_h. The proton-inferred hot electron temperatures for these plasmas are thus 10–20 keV.

It is worth examining how these proton-inferred hot electron temperatures compare to the temperatures found using standard x-ray techniques. In past experiments,[1,2] it was found that the two were in agreement for temperatures of a few keV or below, but for $T_h>10$ keV, the proton-inferred temperatures could be several times lower than those determined from x-ray measurements. Consistent with these pre-

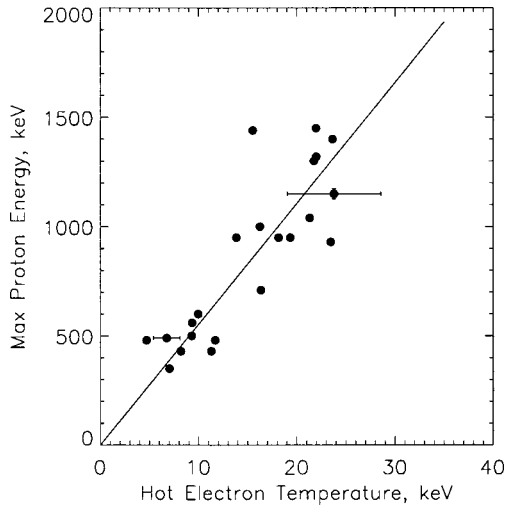

FIG. 3. Maximum proton energy vs the hot electron temperature inferred from the slope of the ion velocity spectrum measured by the CPS. Sample errors bars are shown for two data points. Uncertainties in the inferred temperature are caused by uncertainties in determining the spectral slope. The linear relation is in agreement with that found in previous experiments (Ref. 1).

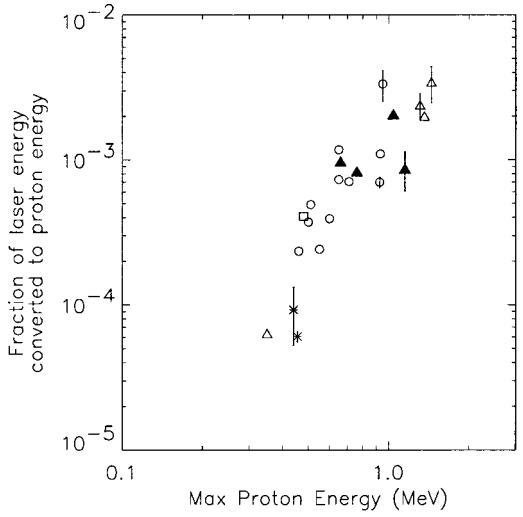

FIG. 4. The fraction of incident laser energy converted to fast protons with energies greater than 0.2 MeV plotted as a function of the maximum proton energy. Plot symbols are as in Fig. 2. Vertical bars on some data points represent the differences between the two spectrometers. In the future, the energy carried by heavier ion species needs to be considered to establish the total amount of laser energy that is converted into kinetic energy of fast ions.

vious findings, concurrent x-ray measurements on our experiments give hot electron temperatures in the range of 50–250 keV. A possible cause for this discrepancy might be the time-evolution of the hot-electron temperature, with the x-ray and proton methods being sensitive to temperatures at different periods during this evolution. Specifically, the ion acceleration is greatest early in the laser pulse when the highest ion densities give rise to the highest space–charge fields.[7] This implies that the proton spectra would weight more heavily the hot electron temperatures existing early in the pulse. On the other hand, hard x-ray measurements are most sensitive to the highest temperatures which generally occur later in the pulse when longer plasma scale lengths allow instabilities to grow. This picture is consistent with the observation that the maximum proton energies are similar on the 0.4 and 1.0 ns pulse length shots, whereas time-resolved x-ray measurements show most of the x-rays on a 1.0 ns shot to be generated after 0.4 ns. The highest energy electrons measured by the x-ray techniques thus may not be responsible for accelerating the ions.

In Fig. 4, the fraction of laser energy converted to fast protons with energies greater than 0.2 MeV is plotted versus the maximum proton energy. The differences between simultaneous measurements on both spectrometers, which are illustrated as vertical bars on some data points, may be as much as a factor of two. This asymmetry in total energy flux is in contrast to the near symmetry in maximum proton energy described above. At $I\lambda^2 = 1.2\times 10^{14}$ $\mathrm{Wcm}^{-2}\mu\mathrm{m}^2$, corresponding to an endpoint of ~ 1 MeV, the total energy carried by the fast protons is $\sim 10^{-3}$ of the laser energy. To within the scatter of the data, protons from the 0.4 ns shots have approximately the same fractional energy as those from the 1 ns shots. This correlation between the energy fraction and the maximum energy, regardless of target material or pulse length, indicates that the maximum proton energy can be used as a rough measure of the total energy in the fast protons. It is noteworthy that, on previous experiments[6] at higher intensities of $I\lambda^2 \sim 10^{17}$ $\mathrm{Wcm}^{-2}\mu\mathrm{m}^2$ where the maximum proton energy was also close to 1 MeV, the fraction of laser energy carried by the fast ions was also $\sim 10^{-3}$.

Also shown in Fig. 1 is a spectrum with oscillations, features that are not repeatable from one shot to the next, and are not necessarily observed on both spectrometers on the same shot. Occasionally, the oscillations take the form of intense lines, as shown in Fig. 5. These lines are generally superimposed upon the exponential-like background spectrum. For a given laser intensity, spectra with or without lines do not show any significant difference in their maximum energy. Such strong spectral lines have not been observed before and, to the best of our knowledge, are not predicted by existing theories.

A common feature amongst all the line spectra is an increase in the spacing between lines going to higher energies. Figure 6 shows that this spacing, when plotted in terms of the velocity difference, ΔV, between two adjacent lines, increases linearly with the average velocity V of the two lines. A simple analysis shows that this increase in line spac-

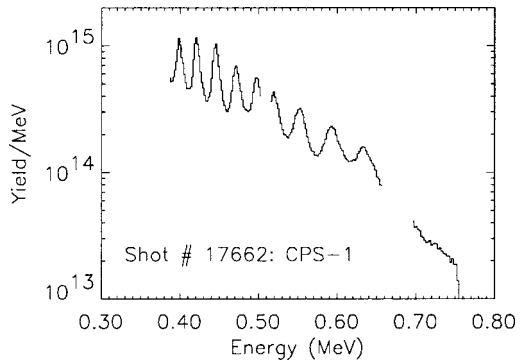

FIG. 5. Occasionally, the proton spectra exhibit discrete lines whose spacing increases with energy. These lines are superimposed upon the exponential-like background.

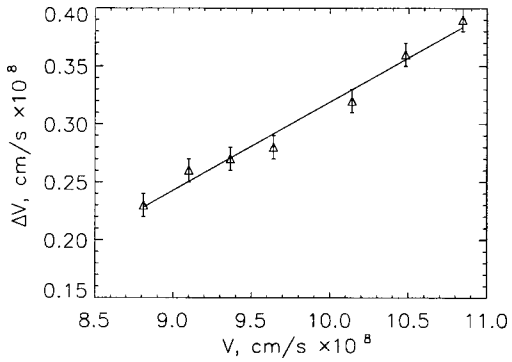

FIG. 6. The difference in velocity, ΔV, between any two adjacent lines in Fig. 5 increases linearly with the average velocity, V, of the two lines.

ing is characteristic of the behavior of a succession of ion acoustic perturbations in an expanding plasma. To see this, consider a plasma moving with background velocity V. Treating the successive ion acoustic perturbations as a single wave, the velocity of such a wave traveling in the same direction as V is simply $u+V$, where u is the wave velocity in the reference frame of the moving plasma. For an expanding plasma, V increases with distance in the direction of the expansion which means that the velocity of successive density peaks in the ion wave will also increase with distance in the expansion direction, producing peaks at different velocities. Using once again the isothermal, self-similar expansion model, where the plasma velocity at a given time is proportional to position, it can be shown that the difference in velocity, ΔV, between successive peaks is given approximately by $\Delta V = 2\pi(u+V)/\omega t$ where ω is the wave frequency and t is the expansion time. Should ωt be constant over this velocity range, ΔV would be proportional to V, as shown in Fig. 6, is well approximated by a straight line. Further studies will be necessary to understand the origin of these perturbations.

IV. CONCLUSIONS AND FURTHER WORK

Fast protons with energies $\gtrsim 1$ MeV have been observed on targets irradiated by the OMEGA, 60-beam laser system—energies more than 5 times greater than observed on past experiments at the same $I\lambda^2$. This substantial enhancement in the ion acceleration is unexpected given the presence of smoothed beams and submicron wavelength laser light on OMEGA. Examining the results of previously reported experiments indicates that the presence of multiple, overlapping beams could play a role in producing such high proton energies. It is interesting that, although the measured maximum proton energies in our studies do not follow the scaling with $I\lambda^2$ found on single-beam experiments in the past, they do follow the scaling with hot electron temperature that was found on such experiments. These temperatures have been determined using the self-similar expansion model for the protons. The total energy in the fast protons above 0.2 MeV has been found to be $\sim 10^{-3}$ of the laser energy. It is likely that a similar, if not greater, fraction of the laser energy could be carried by the heavier fast ions. Occasionally, some spectra show intense lines whose velocity spacing increases linearly with velocity. These lines may be associated with ion acoustic perturbations in the expanding plasma, though their origin is still unclear.

Future experiments should investigate fast proton energies on similar-intensity, single-beam experiments on OMEGA, to determine whether or not multiple beams are responsible for the enhanced ion acceleration. In addition, the time scale of the acceleration process could be determined by examining more closely the sensitivity of the proton spectra to different pulse shapes and pulse rise times. Studying some of the other ions which have been observed—the heavier fast ions as well as the charged fusion products—may also provide further insights into the nature of the acceleration process.

ACKNOWLEDGMENTS

We are indebted to the OMEGA operations group for their expert help. This work was supported in part by LLE Subcontract No. PO410025G, LLNL Subcontract No. B313975, U.S. Department of Energy Contract No. DE-FG03-99SF21782, and the U.S. Department of Energy Office of Inertial Confinement Fusion under Cooperative Agreement No. DE-FC03-92SF19460.

[1] T. H. Tan, G. H. McCall, and A. H. Williams, Phys. Fluids **27**, 296 (1984).
[2] F. N. Beg, A. R. Bell, A. E. Dangor, C. N. Danson, A. P. Fews, M. E. Glinsky, B. A. Hammel, P. Lee, P. A. Norreys, and M. Tatarakis, Phys. Plasmas **4**, 447 (1997).
[3] S. J. Gitomer, R. D. Jones, F. Begay, A. W. Ehler, J. F. Kephart, and R. Kristal, Phys. Fluids **29**, 2679 (1986).
[4] F. Begay and D. W. Forslund, Phys. Fluids **25**, 1675 (1982).
[5] R. Decoste and B. H. Ripin, Phys. Rev. Lett. **40**, 34 (1978).
[6] A. P. Fews, P. A. Norreys, F. N. Beg, A. R. Bell, A. E. Dangor, C. N. Danson, P. Lee, and S. J. Rose, Phys. Rev. Lett. **73**, 1801 (1994).
[7] J. E. Crow, P. L. Auer, and J. E. Allen, J. Plasma Phys. **14**, 65 (1975).
[8] L. M. Wickens, J. E. Allen, and P. T. Rumsby, Phys. Rev. Lett. **41**, 243 (1978).
[9] Y. Kishimoto, K. Mima, T. Watanabe, and K. Nishikawa, Phys. Fluids **26**, 2308 (1983).
[10] E. L. Clark, K. Krushelnick, M. Zepf *et al.*, Phys. Rev. Lett. **85**, 1654 (2000).
[11] T. Ditmire, E. Springate, J. W. G. Tisch, Y. L. Shao, M. B. Mason, N. Hay, J. P. Marangos, and M. H. R. Hutchinson, Phys. Rev. A **57**, 369 (1998).
[12] M. Lezius, S. Dobosz, D. Normand, and M. Schmidt, Phys. Rev. Lett. **80**, 261 (1998).
[13] P. E. Young, G. Guethlein, S. C. Wilks, J. H. Hammer, W. L. Kruer, and K. G. Estabrook, Phys. Rev. Lett. **76**, 3128 (1996).
[14] K. Krushelnick, E. L. Clark, Z. Najmudin *et al.*, Phys. Rev. Lett. **83**, 737 (1999).
[15] T. R. Boehly, D. L. Brown, R. S. Craxton, R. L. Keck, J. P. Knauer, J. H. Kelly, T. J. Kessler, S. A. Kumpan, S. J. Loucks, S. A. Letzring, F. J. Marshall, R. L. McCrory, S. F. B. Morse, W. Seka, J. M. Soures, and C. P. Verdon, Opt. Commun. **133**, 495 (1997).
[16] C. Chan, N. Hershkowitz, A. Ferreira, T. Intrator, B. Nelson, and K. Lonngren, Phys. Fluids **27**, 266 (1984).
[17] S. Skupsky and R. S. Craxton, Phys. Plasmas **6**, 2157 (1999).
[18] D. G. Hicks, C. K. Li, R. D. Petrasso, F. H. Séguin, B. E. Burke, J. P. Knauer, S. Cremer, R. L. Kremens, M. D. Cable, and T. W. Phillips, Rev. Sci. Instrum. **68**, 589 (1997).
[19] D. G. Hicks, C. K. Li, F. H. Séguin, A. K. Ram, R. D. Petrasso, J. M. Soures, V. Yu Glebov, D. D. Meyerhofer, S. Roberts, C. Sorce, C. Stöckl, T. C. Sangster, and T. W. Phillips, Phys. Plasmas **7**, 5106 (2000).
[20] C. K. Li, D. G. Hicks, F. H. Séguin *et al.*, Phys. Plasmas **7**, 2578 (2000).
[21] D. G. Hicks, Ph.D. thesis, Massachusetts Institute of Technology, 1999.
[22] W. Priedhorsky, D. Lier, R. Day, and D. Gerke, Phys. Rev. Lett. **47**, 1661 (1981).